Desalination and Water Treatment
www.deswater.com

doi: 10.1080/19443994.2015.1128982

57 (2016) 22039–22048
October

Taylor & Francis
Taylor & Francis Group

Resin-supported Fe(III) as an efficient heterogeneous Fenton catalyst for degradation of Reactive Black 5

Yan Wang, Yan Chen, Jianfei Wang*, Jiaojiao Lu

Department of Environmental Science and Engineering, Anhui Science and Technology University, Donghua Road 9#, Fengyang 233100, China, Tel. +86 139 65999209; Fax: +86 550 6732317; email: wangyanht@163.com (Y. Wang), Tel. +86 18255007020; Fax: +86 550 6732317; email: 1070064260@qq.com (Y. Chen), Tel. +86 139 55069129; Fax: +86 550 6732317; email: jykwjf@sina.com (J. Wang), Tel. +86 18255005975; Fax: +86 550 6732317; email: 903793853@qq.com (J. Lu)

Received 31 July 2014; Accepted 1 December 2015

ABSTRACT

In this study, a resin-supported Fe(III) catalyst (Fe/R) was developed for the degradation of Reactive Black 5 (RB5) by a heterogeneous Fenton-like reaction. The catalyst stability was evaluated by measuring color removal efficiency for five successive cycles. The Fe/R samples were characterized by XRD, TGA, SEM-EDS, and FTIR techniques as well as physical properties were determined using the BET method. The effect of major parameters including pH, H_2O_2 concentration, catalyst addition, initial dye concentration, reaction temperature, and amount of hydroxyl radical scavenger (*tert*-butyl alcohol) on the decolorization of RB5 was investigated. The results indicated that the RB5 decolorization rate increased with increasing H_2O_2 concentration, reaction temperature, and Fe/R addition, but decreased with increasing initial RB5 concentration, pH, and amount of hydroxyl radical scavenger. The total organic carbon (TOC) removal of RB5 was only 48.6%, and more H_2O_2 was required for TOC further removal.

Keywords: Resin-supported Fe(III); Reactive Black 5; Decolorization; Heterogeneous Fenton-like reaction

1. Introduction

Synthetic dyes are widely used in textile, paper, pharmaceutical, cosmetics, and food industries [1,2]. Approximately 100,000 dyes are synthesized, and over 700,000 tons of synthetic dyes are produced annually [1,3,4]. In particular, the production of synthetic dyes is estimated to be 280,000 tons in China [1]. Moreover, a vast amount of wastewater is generated during the production and utilization of these dyes [1,2,5]. Dyes can inhibit the reoxygenation capacity of water and block sunlight, thus causing environmental damage and disturbing the natural growth of aquatic life [6–9]. Almost 45% of all the textile dyes produced annually belong to azo dyes characterized by one or more azo groups (–N=N–) [2,10,11]. Reactive Black 5 (RB5), as a representative azo dye, is widely used for colorization in textile industries with a relatively high consumption among all the reactive dyes [10,12]. For example, the annual consumption of RB5 in Turkey is 1,000 ton [13,14]. Because of its strong toxicity and carcinogenicity, RB5

*Corresponding author.

and its degradation products threaten the safety of living organisms [10,15]. Moreover, RB5 could not be removed effectively by the traditional methods [16]. Therefore, it is necessary to develop an efficient technique for RB5 wastewater treatment before releasing to the environment.

Recently, advanced oxidation processes (AOPs) have attracted amazing attention for the treatment of organic pollutants in wastewaters due to their high efficiency and fast treatment rate [11]. For example, ozonation [17], Fenton reaction [7,18,19], and other AOPs [11,16,20] have been applied for the removal of azo dyes from effluents. Among these technologies, Fenton oxidation process is promising because of its high efficiency, simple operation, and ability to treat diverse hazardous organics. However, the application of conventional Fenton treatment is limited by its disadvantages such as a tight pH range and large amounts of iron sludge produced after the treatment [21–24].

To overcome these limitations, much effort has been devoted to develop heterogeneous Fenton processes [22]. In heterogeneous Fenton processes, the key is to develop a highly efficient, long life, and low-cost catalyst. Therefore, several catalysts have been developed for this purpose [7,8,12,21,25–27]. But manufacturing of these catalysts requires raw materials and even generates other wastes, such as waste gas, wastewater, and solid wastes [28]. Therefore, the most cost-effective and "green" strategy arguably is the recycling of specific wastes to prepare a catalyst for the degradation of wastewater. In particular, some solid wastes have been used to degrade azo dyes as inexpensive and highly effective active ingredients or carrier of heterogeneous Fenton-like catalysts and taken good catalytic efficiency [12,27–30].

Ion exchange resins are insoluble polymers and have high specific surface area, mechanical properties, and easy separation and able to be exchanged with other ions in solutions. They have been widely used in different industrial processes, such as water softening and purification, juice purification, sugar manufacturing, pharmacy and petrochemical industry [31–33]. After service, a large amount of waste resins are discarded and become a potential threat to the environment. Moreover, the growing concern about environmental pollution and energy shortage makes it urgent necessary to find effective ways for the utilization of waste resins. Some polymeric resins have been successfully utilized as precursors for production of activated carbons [33]. However, waste resin-based Fenton catalysts for the degradation of RB5 have not been reported.

The objective of this study was to develop a new "wastes-treat-wastes" (WTW) technology to prepare a highly effective active catalyst based on waste resin and evaluate its feasibility for the removal of RB5 as heterogeneous Fenton-like catalyst. Therefore, waste cation exchange resin from a thermal power plant in China was selected as the carrier of heterogeneous Fenton-like catalysts and Fe^{3+}, as the reactive ion, was immobilized on the cation exchange resin to develop a stable heterogeneous Fenton-like catalyst, resin-supported Fe(III) (Fe/R). The efficiency and stability of Fe/R for the degradation of RB5 dye in a heterogeneous system were evaluated. The mineralization of RB5 in terms of total organic carbon (TOC) removal and the effects of operating conditions such as Fe/R addition rate, H_2O_2 concentration, initial pH, amount of hydroxyl radical scavenger, and initial dye concentration on color removal were analyzed.

2. Experiment

2.1. Materials

RB5 was purchased from Shanghai Shiyi Chemicals Reagent Co., Ltd (China) and used as received without further purification. H_2O_2 (analytical grade, 30%, w/w) and $FeCl_3$ (99% purity) were obtained from Shanghai Sinopharm Chemical Reagent Co., Ltd. The cation exchange resin was obtained from a thermal power plant in China. All the solutions were prepared with deionized water.

2.2. Preparation and characterization of the catalyst

Fe/R was prepared by wet-impregnation technique using $FeCl_3$ as iron precursor and waste cation exchange resin as carrier. Ten grams of received waste cation exchange resin was soaked in 0.5 mol L^{-1} 100 mL NaOH for 5 h and then filtered and soaked in 0.5 mol L^{-1} 100 mL HCl for 5 h. These were repeated 3 times, and then, the changed resin was washed with deionized water until neutral. A fixed amount of washed resin was added to a 0.05 mol L^{-1} $FeCl_3$ solution, and the suspension was stirred for 24 h at a constant temperature. Then, the sample was filtered and washed with deionized water until neutral. Finally, the sample was dried naturally for 12 h. In order to determine the ratio of ferric ions in the sample, 1 g Fe/R was soaked into a digestion high-pressure tank containing 5 mL 30% (v/v) H_2O_2, 15 mL 98% (v/v) H_2SO_4 and 10 mL concentrated HNO_3. The tank was put into microwave digestion and heated for 10 min. Then, the total amount of iron was evaluated using an atomic absorption spectrometer (AAS, Analytik jena Zeenit 700, Germany).

The morphology and size distribution of Fe/R were analyzed by a scanning electron microscope

(SEM, Zeiss EVO LS-185, UK, operated at 20.0 kV) coupled to an energy-dispersive spectrometer (EDS) for detecting Fe(III) on the sample surface. The particle size distribution of the solid catalyst was measured using a Mastersizer 3500 apparatus (Microtrac, USA). The specific surface area was determined using the BET method (ASAP 2020-M, USA).

The morphology of the catalyst was carried out using a scanning electron microscope (SEM, Zeiss EVO LS-185, UK) operated at 20.0 kV. X-ray diffraction (XRD) patterns were recorded on a D/Max-2550PC diffractometer in θ–2θ configuration to identify the crystal phase and structure. The wide-angle data were collected from 20˚ to 90˚ on 2θ scale, when the operated condition was set at 36 kV/24 mA, using Cu Kα1 radiation with a wavelength of 1.5406 Å.

The thermogravimetric and differential thermal analyses (TGA/DTG) of Fe/R were carried out using a TA Q600 thermogravimetric analyzer (USA). TGA and differential thermal (DTG) curves were obtained under a dynamic atmosphere of N_2 (flow rate of 35 mL min^{-1}) heating rate of 10℃ min^{-1} from 22 to 800℃ with a sample mass of 20.69 mg.

The infrared spectra of synthesized Fe/R were recorded on KBr pellets by a Fourier transform infrared spectrometer (FTIR, Nicolet Avatar 330). To avoid moisture, KBr pellets were prepared by pressing mixtures of dry powered sample and spectrometry-grade KBr under vacuum. A total of 150 scans were collected for each sample in the range of 400–4,000 cm^{-1} with a resolution of 2 cm^{-1}.

2.3. Experimental procedures

All the experiments were performed in beaker containing 200 mL solution. The beaker was immersed into a water bath to keep the temperature around 25℃. A stock solution of RB5 was freshly prepared with deionized water before each run, and the initial concentration was fixed at 50 mg L^{-1}. Unless otherwise specified, the initial pH of the dye solution was adjusted using H_2SO_4 and NaOH. Then, given amounts of H_2O_2 and Fe/R were added into RB5 solution under stirring (150 rpm) using a magnetic stirrer (RW20, IKA, Germany). At preselected time intervals, the samples are removed, filtered through 0.22 μm membranes (Millipore Co.), and immediately mixed with 0.2 mL, 1 mol L^{-1} NaOH solution to quench the reaction before analysis. The absorbance of RB5 was measured at λ_{max} = 591 nm using a Shimadzu UV-1700 spectrophotometer. TOC was analyzed using a TOC analyzer (Shimadzu TOC-L) to evaluate the mineralization of RB5. The total amount of iron leached from Fe/R was evaluated using AAS.

3. Results and discussion

3.1. Catalyst properties

Table 1 shows the physical properties (mean particle diameter, density, BET specific surface area, and average pore diameter) of Fe/R. The specific surface area of Fe/R is 750 m^2 g^{-1} and larger compared with other resin catalysts [34,35]. Thus, it could be believed to be proportional to the number of active sites of the catalyst for reaction processes. The particle size and density also show that Fe/R can be easily separated and recovered after catalysis.

Fe/R was characterized by XRD in high angle range for the crystalline of the loaded ferric ions/iron oxides on the resin and it was depicted in Fig. 1. The poor quality of Fig. 1 may be ascribed to the presence of resin which made the content of ferric ions/iron oxides to be lower and small particles [36]. But wide-angle XRD patterns of Fe/R gave the diffraction peaks that may be indexed well as the formation of iron oxides.

Moreover, the morphology and surface elemental compositions of Fe/R were analyzed by SEM and EDS, respectively. As shown in Fig. 2, Fe/R is the brown spherical particles with a rough morphology and indicates that the iron oxide is immobilized uniformly on the resin surface. The similar phenomena are reported by Zhao et al. [36] and Rakibuddin et al. [37]. In order to illustrate that the iron oxide was immobilized on the resin surface, the quantitative surface compositions of the resin and Fe/R are determined by EDS and the results are shown in Table 2. Iron element was found in the surface of Fe/R and the weight surface concentration of iron was 8.11%, which was consistent with the measured value (7.92%) by AAS. However, no metal elements were found on the surface of the resin. Clearly, iron oxides were successfully immobilized on the surface of the resin. They could not be easily removed from adsorption by agitation.

In order to investigate the thermal stability of the Fe/R catalyst, the reductions of Fe/R are monitored by weight loss and the TG/DTG curves of Fe/R

Table 1
Physical properties of Fe/R

Properties	Values
Grain size (μm)	570–670
Bulk density (g cm^{-3})	0.85
Grain density (g cm^{-3})	1.26
BET surface area (m^2 g^{-1})	750
Average pore diameter (nm)	10

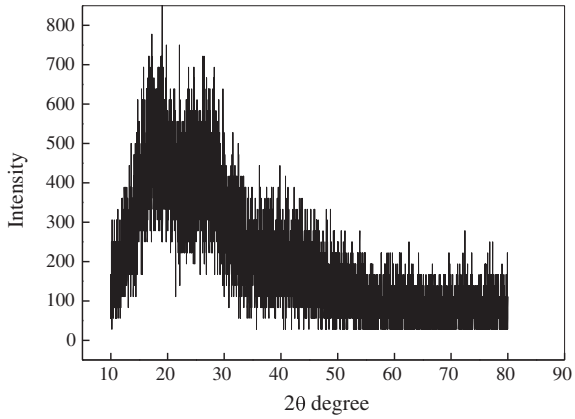

Fig. 1. XRD patterns of Fe/R.

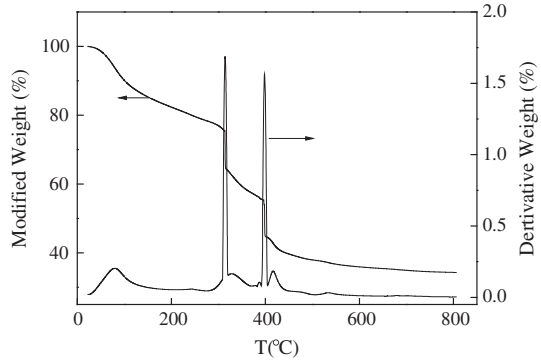

Fig. 3. TG and DTG curves of Fe/R.

catalyst are shown in Fig. 3. As shown in Fig. 3, weight loss for the reduction of Fe/R occurs in three distinct steps. The first loss at 80℃ could be attributed to the removal of physically adsorbed water [38,39]. The weight loss corresponds to this first step constitutes 6.45%. This second stage at 310–319℃ showed a decrease in weight loss comprised of 11.88% due to the carbonization of resin [39]. The third stage indicates weight losses equal 10.78% in the 394–402℃ due to simultaneous condensation of the lattice oxygen and formulation of carbon metals/metallic residues [40].

The FTIR spectra of fresh catalyst are shown in Fig. 4, and various functional groups represented in the FTIR spectra were the same as those of iron oxides. The band between 3,000 and 3,500 cm^{-1} is generated by the stretching of free/bonded hydroxyl

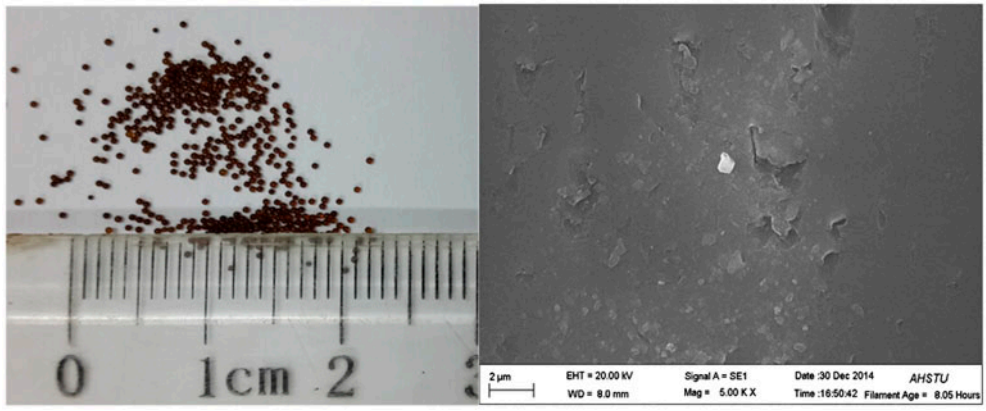

Fig. 2. Fe/R particles and their SEM surface morphology.

Table 2
Surface elemental compositions of resin and Fe/R by EDS

	Resin		Fe/R	
Element	Weight (%)	Atomic (%)	Weight (%)	Atomic (%)
C	49.27	62.34	47.06	61.72
O	30.48	28.68	28.32	27.88
S	20.25	8.98	16.51	8.11
Fe	0	0	8.11	2.29

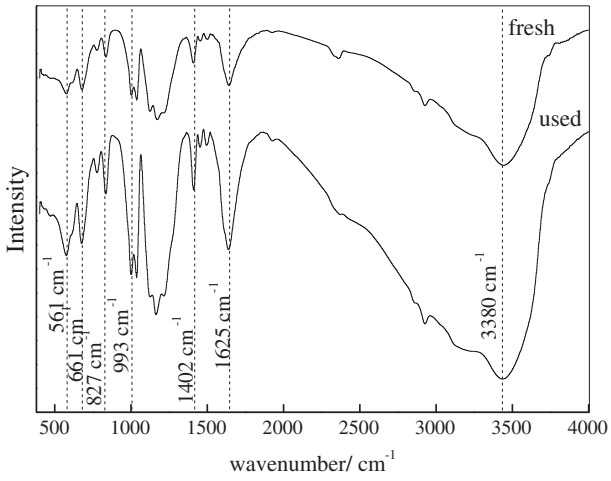

Fig. 4. FTIR spectra of fresh and used Fe/R.

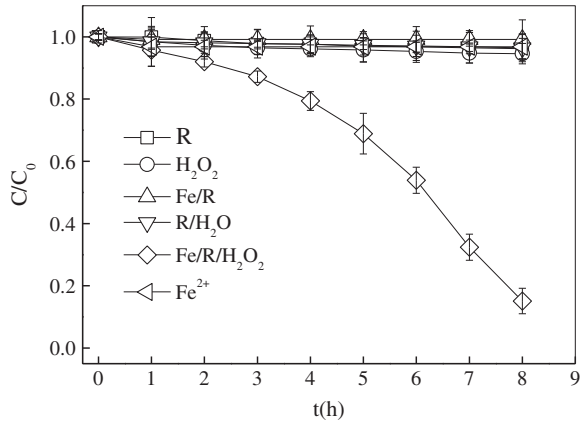

Fig. 5. Degradation of RB5 under different conditions (H_2O_2 = 2 mmol L^{-1}, Fe/R = 2.5 g L^{-1}, Fe^{2+} = 0.13 mg L^{-1}, pH 4, RB5 = 50 mg L^{-1}, temperature = 25°C).

groups [41]. The peaks at about 993 and 995 cm^{-1} are attributed to O–H bending bands in Fe/R (Fe–OH) and are, respectively, on behalf of the vibration in and out of the plane [41]. The band absorption at 661 cm^{-1} is assigned to Fe–O stretching vibrations [41,42]. The bands at 3,446 cm^{-1} are related to the OH vibrations of water molecules [43]. The band at 1,625 cm^{-1} was assigned to the bending vibration of water.

3.2. Degradation of RB5 in different systems

Fig. 5 shows the RB5 decolorization efficiency achieved by different systems. Because of the limited oxidizing power of H_2O_2 (E^0 = 1.77 V vs. NHE), insignificant color removal was observed at ambient temperature after 8-h treatment with H_2O_2 alone. In the control experiments, a slight color removal was observed when the resin or Fe/R was added to the solution alone. Thus, the effect of pretreated resin or Fe/R on RB5 adsorption was not obvious under the conditions of these experiments. This is probably because RB5 is negatively charged due to the presence of sulfonate groups (SO^{3-}) in its structure [2], and the resin surface is also negatively charged. Because of the electrostatic repulsion, RB5 was not adsorbed on the resin surface. Although positively charged Fe(III) ions are adsorbed on the resin surface in Fe/R, the Fe/R surface is not overall positively charged. Thus, neither the resin alone nor Fe/R could adsorb RB5.

Even when H_2O_2 was added to the resin, no significant enhancement in RB5 decolorization was observed, as shown in Fig. 5. Because the resin could not catalyze H_2O_2 to produce ·OH. The Fe/R/H_2O_2 system showed a decolorization efficiency of 84.9%, which was much higher than those obtained under other experimental conditions. Because Fe/R could catalyze H_2O_2 at room temperature to generate ·OH (by the Fenton reaction) and ·OH further oxidized RB5.

Many researchers thought both homogeneous and heterogeneous catalysis were included during iron-based (Fenton reaction) AOPs because of the uncontrolled leaching of iron ions from the catalyst surface [24,44,45]. Therefore, the amount of leaching iron ions was determined and the iron leaching increased gradually during the oxidation process. However, the maximum concentration of the leached iron was approximately 0.13 mg L^{-1}, which can be neglected compared with the standard effluent discharge of 10 mg L^{-1} in China. Moreover, only 3.2% decolorization efficiency could be achieved in the homogeneous Fenton reaction (H_2O_2 = 2 mmol L^{-1}, Fe^{2+} = 0.13 mg L^{-1}, pH 4, RB5 = 50 mg L^{-1}, temperature = 25°C), which was negligible compared to the high decolorization efficiency (84.9%) achieved in the Fe/R/H_2O_2 system, indicating that heterogeneous Fenton reaction played the main role in the Fe/R/H_2O_2 system.

3.3. Stability of Fe/R

The catalytic stability and reusability are important for catalysts. Therefore, the catalytic stability and reusability of Fe/R catalyst were investigated under the following conditions: RB5 concentration = 50 mg L^{-1}, Fe/R addition rate = 2.5 g L^{-1}, H_2O_2 concentration = 2 mmol L^{-1}, reaction temperature = 25°C, and pH 4. The catalyst was filtered and rinsed with deionized water after each experiment and then dried naturally for 12 h. As shown in Fig. 6, 84.9, 83.5, 82.3, 82.5, and 81.9% of RB5 removal rate were obtained in five

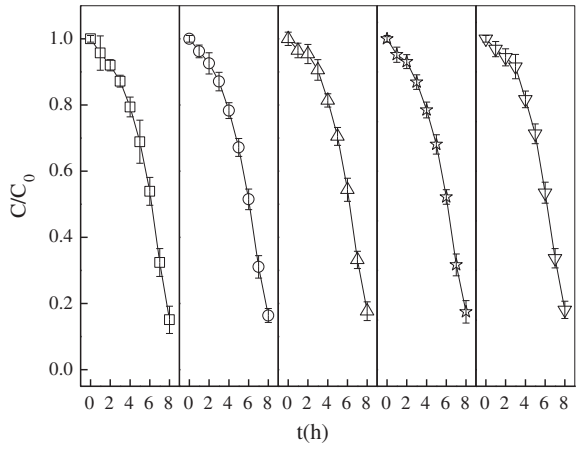

Fig. 6. Reusability of Fe/R (H_2O_2 = 2 mmol L^{-1}, Fe/R = 2.5 g L^{-1}, pH 4, RB5 = 50 mg L^{-1}, temperature = 25°C).

successive cycles. The decolorization efficiencies of RB5 were almost the same in the five successive cycles, indicating that the synthesized Fe/R is an excellent long-term stable catalyst for the Fe/R/H_2O_2 system.

3.4. Effect of the major parameters on RB5 removal

To investigate the effect of initial pH, RB5 solution was treated at various initial pHs (3, 4, 5, 7, and 9) under the following operating conditions: initial RB5 concentration = 50 mg L^{-1}, H_2O_2 concentration = 2 mmol L^{-1}, Fe/R addition = 2.5 g L^{-1}, and temperature = 25°C, respectively. Fig. 7(a) shows that the decolorization efficiency of RB5 decreases from 97.4 to 19.6% when the pH increases from 3 to 9 after 8-h reaction. This result is in agreement with previous studies in the literature [12,27–30,43]. There may be a possible decomposition of H_2O_2 into O_2 and H_2O as well as also the possible deactivation of the catalyst with the formation of the other complexes leading to reduction of ·OH radicals [17,45–47].

Fig. 7(b) shows the decolorization of RB5 at different H_2O_2 concentrations when the initial dye concentration is 50 mg L^{-1}, Fe/R addition is 2.5 g L^{-1}, initial pH value is 4, and temperature is 25°C. As shown in Fig. 7(b), both the decolorization rate and efficiency increased when H_2O_2 concentration increased from 1 to 4 mmol L^{-1}. Because H_2O_2 is the source of ·OH radicals in the Fe/R/H_2O_2 system, and more ·OH radicals are generated to oxidize RB5 at a higher H_2O_2 concentration [23]. A similar phenomenon was reported by Liou et al. [48] when phenol was degraded by heterogeneous oxidation catalysis using resin-supported Fe (III) as the catalyst.

Fig. 7(c) shows the decolorization of RB5 at a Fe/R addition of 1–5 g L^{-1} under the following conditions: pH 4, RB5 concentration = 50 mg L^{-1}, H_2O_2 concentration = 2 mmol L^{-1}, and temperature = 25°C. As shown in Fig. 7(c), the decolorization efficiency of RB5 significantly increased from 34.0 to 99.6% after an 8-h reaction when the Fe/R addition increased from 0.2 to 0.4 g L^{-1}. This is due to the fact that azo dyes are degraded mainly through the heterogeneous Fenton reaction, dependent on the active sites in a specific area of the catalyst [49]. The increase in Fe/R addition corresponds to an increase in the total area, resulting in the faster generation of ·OH radicals from H_2O_2 decomposition by increasing the active sites [48,50]. Thus, the removal rate of organic pollutants increased with increasing Fe/R addition.

As shown in Fig. 7(d), the decolorization efficiency of RB5 increased from 36.3 to 99.8% as the reaction temperature increased from 20 to 65°C. In particular, the decolorization efficiency of RB5 increased rapidly from 46.0 to 96.2% after 1-h reaction when the reaction temperature was increased from 50 to 65°C. It is well known that the decolorization rate is strongly dependent on the ·OH contribution, which usually increases with increasing reaction temperature in the heterogeneous Fenton-like system. However, a higher reaction temperature increased the thermal decomposition rate of H_2O_2 which was not desired. Therefore, the pollutant degradation depended on the competition between thermal decomposition and ·OH formation [48,51]. The results showed that the ·OH formation rate was greater than the thermal H_2O_2 decomposition at high temperatures. Moreover, a higher temperature accelerated the diffusion rate of molecules in solution [52], and increasing the effective collisions between ·OH radicals and RB5, resulting in increased the decolorization rate.

To evaluate the effect of the initial RB5 concentration on the decolorization of RB5, experiments were carried out at various initial RB5 concentrations, and the results were shown in Fig. 7(e). The decolorization rate of RB5 decreased with increasing initial RB5 concentration. Under the constant conditions of the oxidation system such as H_2O_2 concentration and Fe/R addition, the amount and formation rate of ·OH were kept constant when the H_2O_2 concentration and Fe/R addition were unchanged. However, the probability of reaction between azo dye molecules and ·OH decreases with the increase in the initial RB5 concentration [18]. The competition for ·OH radicals among RB5 molecules and their degradation products become pronounced because of the increase in the initial RB5 concentration and nonselective oxidation of ·OH [18,46]. Therefore, the RB5 decolorization rate decreased.

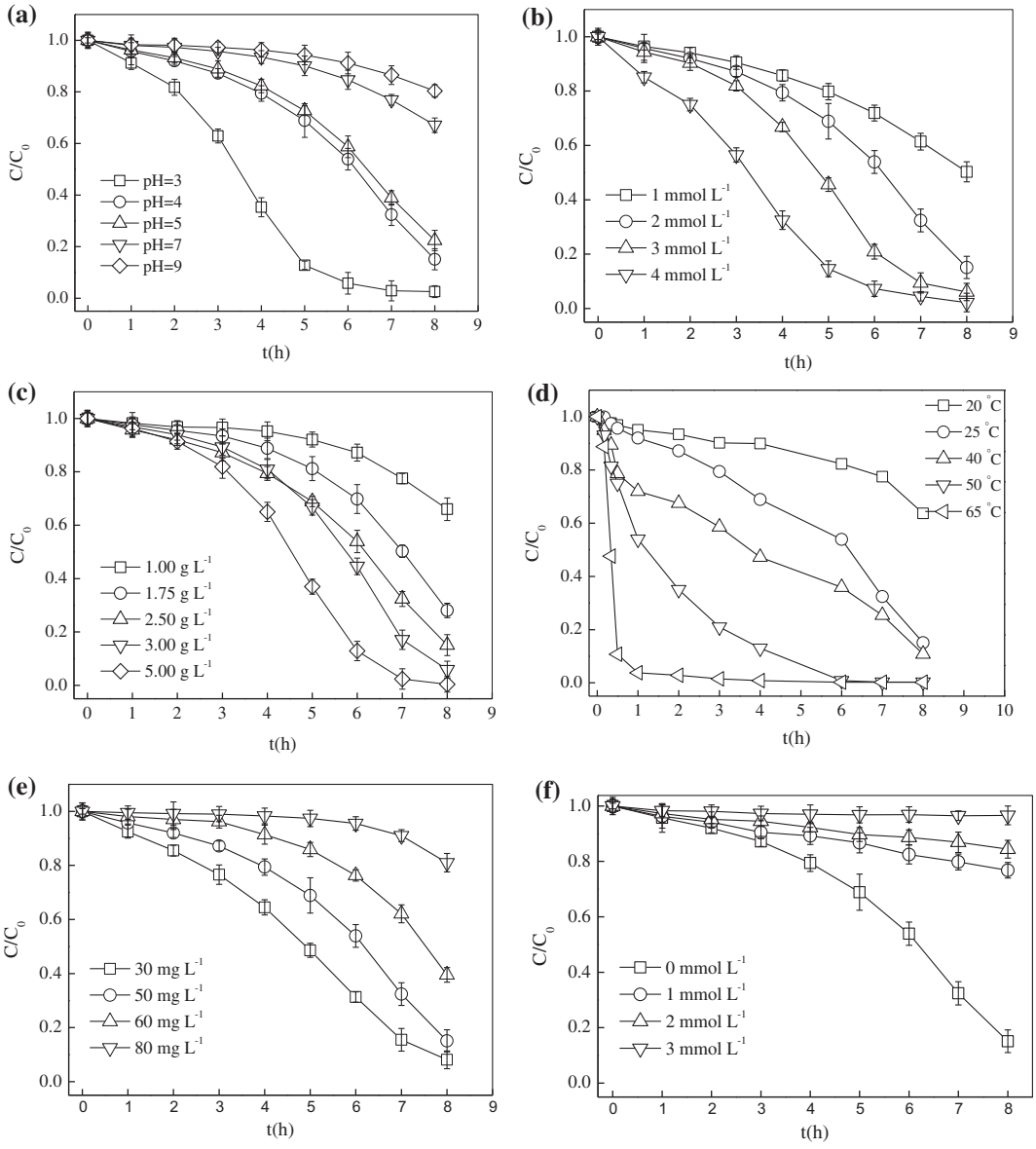

Fig. 7. Effect of operating parameters on the degradation of RB5: (a) pH, (b) H_2O_2 dosage, (c) Fe/R addition, (d) temperature, (e) initial RB5 concentration, and (f) *tert*-butyl alcohol concentration. Except for the investigated parameters, the other parameters were fixed as follows: H_2O_2 = 2 mmol L^{-1}, Fe/R = 2.5 g L^{-1}, pH 4, RB5 = 50 mg L^{-1}, and temperature = 25°C.

A previous report revealed that dye degradation mainly depended on the generation of ·OH that attacked the diazo bonds of azo dyes in the heterogeneous Fenton-like system [18,53]. To further investigate whether the ·OH oxidation was the major mechanism for the decolorization of RB5, experiments were conducted in the presence of *tert*-butyl alcohol, a strong hydroxyl radical scavenger [54,55]. The obvious inhibitory effect of *tert*-butyl alcohol concentration on the decolorization rates of RB5 is shown in Fig. 7(f). The decolorization rate decreased with increasing dosage of *tert*-butyl alcohol and it tended to zero when *tert*-butyl alcohol concentration reached 3 mmol L^{-1}, indicating that the RB5 decolorization was mainly contributed by ·OH oxidation.

3.5. Decolorization and mineralization of RB5 with reaction time

The complete decolorization of RB5 does not mean that the dye is completely oxidized to CO_2, H_2O, and NO_3^- [18,49]. Therefore, the mineralization tests were

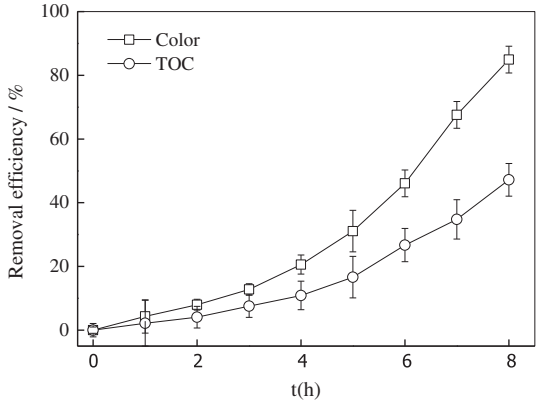

Fig. 8. Decolorization and mineralization of RB5 with reaction time (H_2O_2 = 2 mmol L^{-1}, Fe/R = 2.5 g L^{-1}, pH 4, RB5 = 50 mg L^{-1}, temperature = 25°C).

determined before and after degradation of RB5 by Fe/R H_2O_2. As shown in Fig. 8, less than 26.7% TOC was removed after 6-h reaction compared with 46.1% RB5 decolorization efficiency under the following conditions: initial dye concentration = 50 mg L^{-1}, H_2O_2 concentration = 2 mmol L^{-1}, Fe/R addition rate = 2.5 g L^{-1}, and pH 4. When the decolorization of RB5 nearly reached 85% after 8-h reaction, the TOC removal rate was still less than 50%. It was the fact that only 0.05 mmol L^{-1} H_2O_2 was theoretically needed to completely bleach 50 mg L^{-1} RB5 based on the following mechanism suggested for the RB5 decolorization, taking into account Eq. (1) [45,55]:

$$C_{26}H_{21}N_5Na_4O_{19}S_6 + {}^{\cdot}OH \rightarrow C_{16}H_{10}N_2Na_2O_7S_2(\text{–OH}) + \text{oxidized intermediates} \quad (1)$$

A known value of 2 mmol L^{-1} H_2O_2 was sufficient for RB5 decolorization in the Fe/R/H_2O_2 system. Based on the report proposed by Zhang [49], the complete mineralization of RB5 could be described by Eq. (2) below:

$$C_{26}H_{21}N_5Na_4O_{19}S_6 + 82.5H_2O_2 \rightarrow 26CO_2 + 5NO_3^- + 6SO_4^{2-} + 4Na^+ + 93H_2O \quad (2)$$

According to this equation, 4.2 mmol L^{-1} of H_2O_2 is theoretically needed to completely degrade 50 mg L^{-1} of RB5 and as high as two times H_2O_2 addition used in this study. Thus, only 48.6% TOC was removed, whereas 84.9% degradation efficiency was achieved under the same conditions, and a further increase in reaction time and more H_2O_2 might increase TOC removal.

4. Conclusion

The results indicate that Fe/R, as an efficient catalyst, can catalyze efficiently H_2O_2 to generate ·OH for the degradation of RB5. The ratio of ferric ions in Fe/R was 7.92%. The leached iron (0.13 mg L^{-1}) from Fe/R and the effect of homogeneous Fenton oxidation on the RB5 degradation can be neglected. The increase in Fe/R addition rate, H_2O_2 concentration, and reaction temperature increased the degradation rate and degradation efficiency. In contrast, the degradation rate and degradation efficiency decreased with the increase in pH and initial RB5 concentration. The presence of a hydroxyl radical scavenger (*tert*-butyl alcohol) hindered the degradation reaction. Decolorization rate reached 84.9% under the operating condition (H_2O_2 = 2 mmol L^{-1}, Fe/R = 2.5 g L^{-1}, pH 4, RB5 = 50 mg L^{-1}, temperature = 25°C), but only 48.6% TOC was removed. To achieve higher TOC removal, a further increase in reaction time or more H_2O_2 is required.

Acknowledgment

This study was supported by the Anhui Science and Technology University Talents Introduction Foundation (Grant No. ZRC2012328).

References

[1] Z.W. Wang, J.S. Liang, Y. Liang, Decolorization of Reactive Black 5 by a newly isolated bacterium *Bacillus* sp. YZU1, Int. Biodeterior. Biodegrad. 76 (2013) 41–48.
[2] A. Nematollahzadeh, A. Shojaei, M. Karimi, Chemically modified organic/inorganic nanoporous composite particles for the adsorption of reactive black 5 from aqueous solution, React. Funct. Polym. 86 (2015) 7–15.
[3] L. Guz, G. Curutchet, R.M. Torres Sánchez, R. Candal, Adsorption of crystal violet on montmorillonite (or iron modified montmorillonite) followed by degradation through Fenton or photo-Fenton type reactions, J. Environ. Chem. Eng. 2 (2014) 2344–2351.
[4] G.M. Nabil, N.M. El-Mallah, M.E. Mahmoud, Enhanced decolorization of reactive black 5 dye by active carbon sorbent-immobilized-cationic surfactant (AC-CS), J. Ind. Eng. Chem. 20 (2014) 994–1002.
[5] M.L. Rache, A.R. García, H.R. Zea, A.M.T. Silva, L.M. Madeira, J.H. Ramírez, Azo-dye orange II degradation by the heterogeneous Fenton-like process using a zeolite Y-Fe catalyst—Kinetics with a model based on the Fermi's equation, Appl. Catal. B: Environ. 146 (2014) 192–200.

[6] M. Siddique, R. Farooq, G.J. Price, Synergistic effects of combining ultrasound with the Fenton process in the degradation of Reactive Blue 19, Ultrason. Sonochem. 21 (2014) 1206–1212.
[7] H.H. Wu, X.W. Dou, D.Y. Deng, Y.F. Guan, L.G. Zhang, G.P. He, Decolourization of the azo dye Orange G in aqueous solution via a heterogeneous Fenton-like reaction catalysed by goethite, Environ. Technol. 33 (2012) 1545–1552.
[8] M.A. Kamboh, I.B. Solangi, S.T.H. Sherazi, S. Memon, A highly efficient calix[4]arene based resin for the removal of azo dyes, Desalination 268 (2011) 83–89.
[9] M.S. Lucas, P.B. Tavares, J.A. Peres, J.L. Faria, M. Rocha, C. Pereira, C. Freire, Photocatalytic degradation of Reactive Black 5 with TiO_2-coated magnetic nanoparticles, Catal. Today 209 (2013) 116–121.
[10] M.H. Kim, C.H. Hwang, S.B. Kang, S. Kim, S.W. Park, Y.S. Yun, S.W. Won, Removal of hydrolyzed Reactive Black 5 from aqueous solution using a polyethylenimine–polyvinyl chloride composite fiber, Chem. Eng. J. 280 (2015) 18–25.
[11] H. Lin, H. Zhang, X. Wang, L.G. Wang, J. Wu, Electro-Fenton removal of Orange II in a divided cell: Reaction mechanism, degradation pathway and toxicity evolution, Sep. Purif. Technol. 122 (2014) 533–540.
[12] G. Ersöz, Fenton-like oxidation of Reactive Black 5 using rice husk ash based catalyst, Appl. Catal. B: Environ. 147 (2014) 353–358.
[13] İ.A. Şengil, M. Özacar, The decolorization of C.I. Reactive Black 5 in aqueous solution by electrocoagulation using sacrificial iron electrodes, J. Hazard. Mater. 161 (2009) 1369–1376.
[14] I.A. Alaton, I.A. Balcioglu, Photochemical and heterogeneous photocatalytic degradation of waste vinylsulphone dyes: A case study with hydrolyzed Reactive Black 5, J. Photochem. Photobiol., A 141 (2001) 247–254.
[15] M. Işık, D.T. Sponza, A batch kinetic study on decolorization and inhibition of Reactive Black 5 and Direct Brown 2 in an anaerobic mixed culture, Chemosphere 55 (2004) 119–128.
[16] X. Wang, L.G. Wang, J.B. Li, J.J. Qiu, C. Cai, H. Zhang, Degradation of Acid Orange 7 by persulfate activated with zero valent iron in the presence of ultrasonic irradiation, Sep. Purif. Technol. 122 (2014) 41–46.
[17] G.G. Bessegato, J.C. Cardoso, B.F. da Silva, M.V.B. Zanoni, Combination of photoelectrocatalysis and ozonation: A novel and powerful approach applied in Acid Yellow 1 mineralization, Appl. Catal. B: Environ. 180 (2016) 161–168.
[18] Y.W. Gao, Y. Wang, H. Zhang, Removal of Rhodamine B with Fe-supported bentonite as heterogeneous photo-Fenton catalyst under visible irradiation, Appl. Catal. B: Environ. 178 (2015) 29–36.
[19] V. Dulman, S.M. Cucu-Man, R.I. Olariu, R. Buhaceanu, M. Dumitraş, I. Bunia, A new heterogeneous catalytic system for decolorization and mineralization of Orange G acid dye based on hydrogen peroxide and a macroporous chelating polymer, Dyes Pigm. 95 (2012) 79–88.
[20] C. Cai, L.G. Wang, H. Gao, L.W. Hou, H. Zhang, Ultrasound enhanced heterogeneous activation of peroxydisulfate by bimetallic Fe-Co/GAC catalyst for the degradation of Acid Orange 7 in water, J. Environ. Sci. 26 (2014) 1267–1273.
[21] X.Y. Zhang, Y.B. Ding, H.Q. Tang, X.Y. Han, Degradation of bisphenol A by hydrogen peroxide activated with $CuFeO_2$ microparticles as a heterogeneous Fenton-like catalyst: Efficiency, stability and mechanism, Chem. Eng. J. 236 (2014) 251–262.
[22] L. Djeffal, S. Abderrahmane, M. Benzina, S. Siffert, S. Fourmentin, Efficiency of natural clay as heterogeneous Fenton and photo-Fenton catalyst for phenol and tyrosol degradation, Desalin. Water Treat. 52 (2014) 2225–2230.
[23] Q. Wang, S.L. Tian, J. Cun, P. Ning, Degradation of methylene blue using a heterogeneous Fenton process catalyzed by ferrocene, Desalin. Water Treat. 51 (2013) 5821–5830.
[24] X.N. Fei, W.Q. Li, L.Y. Cao, J.H. Zhao, Y. Xia, Degradation of bromamine acid by a heterogeneous Fenton-like catalyst Fe/Mn supported on sepiolite, Desalin. Water Treat. 51 (2013) 4750–4757.
[25] C.H. Weng, Y.T. Lin, H.M. Yuan, Rapid decoloration of Reactive Black 5 by an advanced Fenton process in conjunction with ultrasound, Sep. Purif. Technol. 117 (2013) 75–82.
[26] A.D. Bokare, W.Y. Choi, Review of iron-free Fenton-like systems for activating H_2O_2 in advanced oxidation processes, J. Hazard. Mater. 275 (2014) 121–135.
[27] X.J. Lv, Y.M. Xu, K. Lv, G.C. Zhang, Photo-assisted degradation of anionic and cationic dyes over iron (III)-loaded resin in the presence of hydrogen peroxide, J. Photochem. Photobiol., A 173 (2005) 121–127.
[28] A.A. Aly, Y.N.Y. Hasan, A.S. Al-Farraj, Olive mill wastewater treatment using a simple zeolite-based low-cost method, J. Environ. Manage. 145 (2014) 341–348.
[29] Y. Wang, R. Priambodo, H. Zhang, Y.-H. Huang, Degradation of the azo dye Orange G in a fluidized bed reactor using iron oxide as a heterogeneous photo-Fenton catalyst, RSC Adv. 5 (2015) 45276–45283.
[30] Y. Li, F.S. Zhang, Catalytic oxidation of Methyl Orange by an amorphous FeOOH catalyst developed from a high iron-containing fly ash, Chem. Eng. J. 158 (2010) 148–153.
[31] T.T. Liu, C.H. Ma, X.Y. Sui, L. Yang, Y.G. Zu, C.J. Zhao, C.Y. Li, L. Zhang, Preparation of shikonin by hydrolyzing ester derivatives using basic anion ion exchange resin as solid catalyst, Ind. Crops Prod. 36 (2012) 47–53.
[32] G.W. Zhou, W.Q. Zhong, H.C. Zhao, B.S. Jin, T.C. Wang, F. Liu, Heat transfer of spent ion exchange resin in iron ore sintering process, Appl. Therm. Eng. 88 (2015) 258–264.
[33] Q.Q. Shi, A.M. Li, Z.L. Zhu, B. Liu, Adsorption of naphthalene onto a high-surface-area carbon from waste ion exchange resin, J. Environ. Sci. 25 (2013) 188–194.
[34] J.Y. Fu, L.G. Chen, P.M. Lv, L.M. Yang, Z.H. Yuan, Free fatty acids esterification for biodiesel production using self-synthesized macroporous cation exchange resin as solid acid catalyst, Fuel 154 (2015) 1–8.
[35] B.M. Antunes, A.E. Rodrigues, Z. Lin, I. Portugal, C.M. Silva, Alkenes oligomerization with resin catalysts, Fuel Process. Technol. 138 (2015) 86–99.
[36] Y.P. Zhao, J.Y. Hu, H.B. Chen, Elimination of estrogen and its estrogenicity by heterogeneous photo-Fenton

catalyst β-FeOOH/resin, J. Photochem. Photobiol., A 212 (2010) 94–100.
[37] M. Rakibuddin, S. Gazi, R. Ananthakrishnan, Iron(II) phenanthroline-resin hybrid as a visible light-driven heterogeneous catalyst for green oxidative degradation of organic dye, Catal. Commun. 58 (2015) 53–58.
[38] I. Ibrahim, I.O. Ali, T.M. Salama, A.A. Bahgat, M.M. Mohamed, Synthesis of magnetically recyclable spinel ferrite (MFe_2O_4, M = Zn, Co, Mn) nanocrystals engineered by sol gel-hydrothermal technology: High catalytic performances for nitroarenes reduction, Appl. Catal. B: Environ. 181 (2016) 389–402.
[39] G.F. Leal, L.A. Ramos, D.H. Barrett, A.A.S. Curvelo, C.B. Rodella, A thermogravimetric analysis (TGA) method to determine the catalytic conversion of cellulose from carbon-supported hydrogenolysis process, Thermochim. Acta 616 (2015) 9–13.
[40] L.J. Ma, R. Wu, H.D. Liu, W.J. Xu, L.S. Chen, S.Y. Chen, Studies on CO_2 decomposition over H_2-reduced MFe_2O_4 (M = Ni, Cu, Co, Zn), Solid State Sci. 13 (2011) 2172–2176.
[41] L.C.A. Oliveira, T.C. Ramalho, E.F. Souza, M. Gonçalves, D.Q.L. Oliveira, M.C. Pereira, J.D. Fabris, Catalytic properties of goethite prepared in the presence of Nb on oxidation reactions in water: Computational and experimental studies, Appl. Catal. B: Environ. 83 (2008) 169–176.
[42] N. Sankararamakrishnan, A. Gupta, S.R. Vidyarthi, Enhanced arsenic removal at neutral pH using functionalized multiwalled carbon nanotubes, J. Environ. Chem. Eng. 2 (2014) 802–810.
[43] Y. Wang, Y.W. Gao, L. Chen, H. Zhang, Goethite as an efficient heterogeneous Fenton catalyst for the degradation of methyl orange, Catal. Today 252 (2015) 107–112.
[44] S.R. Pouran, A.A.A. Raman, W.M.A.W. Daud, Review on the application of modified iron oxides as heterogeneous catalysts in Fenton reactions, J. Cleaner Prod. 64 (2014) 24–35.
[45] F. Duan, Y.Z. Yang, Y.P. Li, H.B. Cao, Y. Wang, Y. Zhang, Heterogeneous Fenton-like degradation of 4-chlorophenol using iron/ordered mesoporous carbon catalyst, J. Environ. Sci. 26 (2014) 1171–1179.
[46] S.X. Zha, Y. Cheng, Y. Gao, Z.L. Chen, M. Megharaj, R. Naidu, Nanoscale zero-valent iron as a catalyst for heterogeneous Fenton oxidation of amoxicillin, Chem. Eng. J. 255 (2014) 141–148.
[47] B.Z. Li, J. Zhu, Removal of p-chloronitrobenzene from groundwater: Effectiveness and degradation mechanism of a heterogeneous nanoparticulate zero-valent iron (NZVI)-induced Fenton process, Chem. Eng. J. 255 (2014) 225–232.
[48] R.M. Liou, S.H. Chen, M.Y. Hung, C.S. Hsu, J.Y. Lai, Fe(III) supported on resin as effective catalyst for the heterogeneous oxidation of phenol in aqueous solution, Chemosphere 59 (2005) 117–125.
[49] H. Zhang, F. Liu, X.G. Wu, J.H. Zhang, D.B. Zhang, Degradation of tetracycline in aqueous medium by electrochemical method, Asia-Pac. J. Chem. Eng. 4 (2009) 568–573.
[50] Y. Wang, H. Zhang, L. Chen, Ultrasound enhanced catalytic ozonation of tetracycline in a rectangular air-lift reactor, Catal. Today 175 (2011) 283–292.
[51] F. Velichkova, C. Julcour-Lebigue, B. Koumanova, H. Delmas, Heterogeneous Fenton oxidation of paracetamol using iron oxide (nano)particles, J. Environ. Chem. Eng. 1 (2013) 1214–1222.
[52] Y. Wang, H. Zhang, L. Chen, S. Wang, D.B. Zhang, Ozonation combined with ultrasound for the degradation of tetracycline in a rectangular air-lift reactor, Sep. Purif. Technol. 84 (2012) 138–146.
[53] M. Muruganandham, J.S. Yang, J.J. Wu, Effect of ultrasonic irradiation on the catalytic activity and stability of goethite catalyst in the presence of H_2O_2 at acidic medium, Ind. Eng. Chem. Res. 46 (2007) 691–698.
[54] G.V. Buxton, C.L. Greenstock, W.P. Helman, A.B. Ross, Critical review of rate constants for reaction of hydrated electrons, hydrogen atoms and hydroxyl radicals (•OH/•O−) in aqueous solution, J. Phys. Chem. Ref. Data 17 (1988) 513–886.
[55] Y. Wang, H. Zhang, J.H. Zhang, L. Chen, Q.Q. Huang, J. Wu, F. Liu, Degradation of tetracycline in aqueous media by ozonation in an internal loop-lift reactor, J. Hazard. Mater. 192 (2011) 35–43.